Canadian Science Publishing

ARTICLE

Efficient separation of propylene and propane on SAPO-17 molecular sieve

Yansi Tong, Jiacheng Xing, Caiyi Lou, Danhua Yuan, Wei Huang, Zhaoan Chen, Zhongmin Liu, and Yunpeng Xu

Abstract: In this study, the separation performance of propylene and propane on SAPO-17 molecular sieve was investigated by static and dynamic adsorption. The adsorbent possessed good regeneration behavior because the strong adsorption of propylene at room temperature was eliminated by ion exchange treatment. Dynamic adsorption experiments revealed that the kinetic separation selectivity of propylene and propane was as high as 1980, which could be attributed to the energy barrier difference when diffusing through the eight-membered ring of SAPO-17 molecular sieve. The breakthrough experiments verified the good separation performance of the SAPO-17 adsorbent, which suggests that it has considerable application potential in propylene/propane separation.

Key words: kinetic separation, silicoaluminophosphate, propylene and propane, ion exchange.

Résumé : Dans le cadre de la présente étude, nous avons étudié la performance de séparation du propylène et du propane sur le tamis moléculaire SAPO17 par adsorption statique et dynamique. L'adsorbant a montré un bon comportement de régénération, le propylène fortement adsorbé à température ambiante ayant été éliminé au moyen d'un traitement par échange d'ions. Des expériences d'adsorption dynamique ont révélé que la sélectivité de séparation cinétique du propylène et du propane atteignait 1 980, ce qui pourrait s'expliquer par la différence de barrière énergétique lors de la diffusion dans le cycle à 8 membres du tamis moléculaire SAPO17. Ces expériences constituent une percée, car elles ont permis de vérifier la bonne performance de séparation du SAPO17, ce qui laisse entrevoir le potentiel considérable d'application de cet adsorbant à la séparation du propylène et du propane. [Traduit par la Rédaction]

Mots-clés : séparation cinétique, silicoaluminophosphate, propylène et propane, échange d'ions.

1. Introduction

As a vital feedstock for the production of polypropylene, polycarbonate, polyacrylonitrile, and polyurethane, the market demand for polymer-grade propylene is considerable.[1,2] The separation of propylene and its paraffin counterpart propane is a research topic that possesses theoretical value and practical significance. Cryogenic distillation is the dominant technology for propylene/propane separation,[3] which is operationally demanding and energy intensive because the boiling points of this gas pair are similar.[4,5] Adsorptive separation is proposed as a more energy efficient alternative method for propylene/propane separation,[6] and molecular sieves are considered promising candidate adsorbents because of their ordered channel structures and thermal stability.[7,8]

Molecular sieves have been widely studied for propylene/propane separation, and aluminosilicate zeolites 13X and 4A are the earliest examples. Owing to the highly polarized environments in these zeolites, propylene with greater dipole moment tends to have a stronger interaction with these adsorbents.[9] The pure-component, binary adsorption, and fixed bed adsorption experiments results[10,11] show that propylene has larger adsorption capacity than propane on 13X. The vacuum swing adsorption (VSA)[12] and simulated moving bed (SMB)[13] separation processes using this adsorbent are supposed to produce polymer-grade propylene. For 4A zeolite, the equilibrium adsorption capacity of propane is lower than propylene;[10] moreover, the diffusion rate of propane is much smaller than propylene.[14] The consistent equilibrium and kinetic selectivity make 4A zeolite a potential adsorbent for effective propylene/propane separation. In recent decades, small pore molecular sieves with eight-membered channels attract most researchers' attentions because their pore sizes are in a similar range to the molecular diameters of propylene and propane. Pure-silica zeolite DD3R,[15,16] ITQ-3,[17] ITQ-12,[18] ITQ-32,[19] Si-CHA,[17] aluminophosphate molecular sieve AlPO-14,[20] and high-silica zeolite ZSM-58[17] exhibit good performance in kinetic separation of propylene and propane mixtures due to their unique pore structures. In spite of their high separation selectivities, the application potentials of above adsorbent materials are inhibited by the high costs and difficulties in the synthesis process. Thus, research on molecular sieves that are more inexpensive and obtainable, such as silicoaluminophosphate, is of

Received 3 December 2020. Accepted 24 January 2021.

Y. Tong, J. Xing, and C. Lou. National Engineering Laboratory for Methanol to Olefins, Dalian National Laboratory for Clean Energy, Dalian Institute of Chemical Physics, Chinese Academy of Sciences, Dalian 116023, China; University of Chinese Academy of Sciences, Beijing 100049, China.
D. Yuan, W. Huang, Z. Chen, and Y. Xu. National Engineering Laboratory for Methanol to Olefins, Dalian National Laboratory for Clean Energy, Dalian Institute of Chemical Physics, Chinese Academy of Sciences, Dalian 116023, China.
Z. Liu. National Engineering Laboratory for Methanol to Olefins, Dalian National Laboratory for Clean Energy, Dalian Institute of Chemical Physics, Chinese Academy of Sciences, Dalian 116023, China; University of Chinese Academy of Sciences, Beijing 100049, China; State Key Laboratory of Catalysis, Dalian Institute of Chemical Physics, Chinese Academy of Sciences, Dalian 116023, China.

Corresponding author: Yunpeng Xu (email: xuyunpeng@dicp.ac.cn).

Fig. 1. (*a*) XRD patterns of (*i*) simulated ERI zeolite, (*ii*) as-synthesized SAPO-17, (*iii*) H-SAPO-17, and (*iv*) Na-SAPO-17. (*b*) N_2 adsorption isotherms of samples at 77 K. Closed symbols, adsorption; open symbols, desorption. [Colour online.]

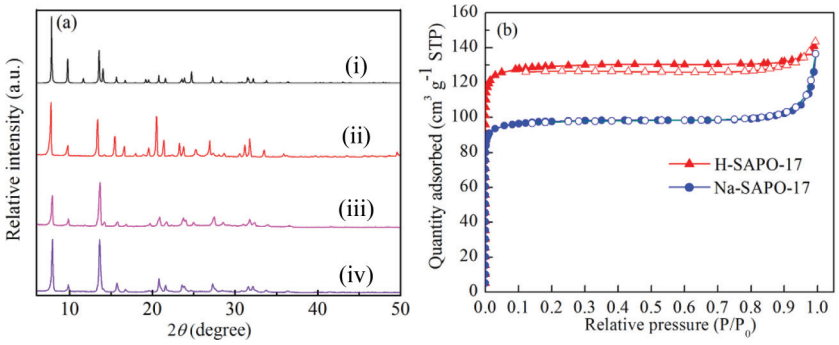

great importance and urgency. Compared with the topological isomorphism, the synthesis process of silicoaluminophosphate molecular sieve is usually easier and more environmentally friendly. Moreover, the negatively charged framework of silicoaluminophosphate molecular sieve make it possible to tune the channel dimension by introducing different cations via ion exchange.[21,22]

SAPO-17 is a silicoaluminophosphate molecular sieve with an ERI topological structure. The channels of the SAPO-17 molecular sieve are connected by eight-membered rings, and the aperture is 3.6 Å × 5.1 Å,[23] similar to the molecular diameters of propylene and propane. In this work, low-silica SAPO-17 with high crystallinity was successfully synthesized and then treated by calcination and ion exchange process to obtain two absorbents, proton form SAPO-17 (H-SAPO-17) and sodium form SAPO-17 (Na-SAPO-17). The samples were systematically characterized by means of XRD, XRF, SEM, ^{1}H NMR, IR, etc. The propylene/propane adsorption and separation performances were tested by the static volumetric method, dynamic gravimetric method, breakthrough experiments, etc.

2. Experimental

2.1. Reagents and characterizations

Aluminum isopropoxide (AIP, 98%) and cyclohexylamine (CHA, 99.5%) were purchased from Shanghai Aladdin Reagent Co., China. Phosphonic acid (H_3PO_4, 85%) was purchased from Tianjin Damao Reagent Co., China. Tetraethyl orthosilicate (TEOS, 98%) was purchased from Tianjin Kermel Reagent Co., China. Sodium chloride (NaCl, 99.5%) was purchased from Tianjin Tianda Chemical Reagent Co., China.

A PANalytical X'Pert PRO X-ray diffractometer with Cu-Kα radiation (λ = 1.54059 Å) was used to record powder X-ray diffraction (XRD) patterns, operating at 40 kV and 40 mA. A Philips Magix-601 X-ray fluorescence (XRF) spectrometer was used to determine the chemical composition of the samples. Field emission scanning electron microscopy (SEM, Hitachi SU8020) was used to observe the morphology of samples. A Bruker Avance III-600 solid-phase NMR spectrometer with a 4 mm probe head was used to record ^{1}H NMR spectra of samples. Bruker Tensor 27 instrument was used to record the infrared spectra of samples. The micropore properties of samples were analyzed by N_2 sorption on a Micromeritics ASAP 2020 volumetric adsorption analyzer at 77 K. The surface area was calculated based on Brunauer–Emmett–Teller (BET) equation, P/P_0 in the range of 0.05~0.3. Micropore volume was calculated by the t-plot method. A Micromeritics ASAP 2050 volumetric adsorption analyzer with 298 K water bath was used to measure the equilibrium adsorption capacities of propylene and propane on samples. In the regeneration experiment, the tested sample was vacuumed on the pretreatment station at room temperature for 10 h. The adsorption kinetics of pure component adsorbate were measured on a Hiden Isochema intelligent gravitation analyzer (IGA100); the operating pressure was 5 mbar, and the temperature was 298 K.

Table 1. Textural properties of H-SAPO-17 and Na-SAPO-17.

	Surface area ($m^2\ g^{-1}$)			Pore volume ($m^3\ g^{-1}$)	
Sample	S_{total}	S_{micro}	S_{ext}	V_{total}	V_{micro}
H-SAPO-17	414	382	31	0.21	0.19
Na-SAPO-17	312	286	25	0.18	0.14

Note: S_{total}, BET surface area; S_{micro}, t-plot micropore area; S_{ext}, t-plot external surface area; V_{total}, total pore volume; V_{micro}, t-plot micropore volume.

2.2. Synthesis and modification of the SAPO-17 molecular sieve

The SAPO-17 molecular sieve was synthesized according to US patent 4440871.[24] Phosphonic acid (4.61 g), aluminum isopropoxide (8.16 g), and deionized water (18.0 g) were mixed and stirred at 323 K for 1 h until homogeneous. Tetraethyl orthosilicate (0.42 g) was added to the above mixture and stirred for another 0.5 h. Finally, cyclohexylamine (1.98 g) was added to the colloid dropwise. The composition of the reaction mixture was 1 Al_2O_3 : 1 P_2O_5 : 0.1 SiO_2 : 1 CHA : 50 H_2O.

After stirring for 0.5 h, the homogeneous mixture was transferred to an autoclave and crystallized at 473 K for 96 h under autogenous pressure and tumbling conditions. After cooling to room temperature, the solid products were filtered out, washed with deionized water, and then dried at 393 K. The templates in as-synthesized SAPO-17 were removed by calcination at 873 K for 6 h. The obtained template-free molecular sieve SAPO-17 (H-SAPO-17) was modified as a Na-type molecular sieve (Na-SAPO-17) by three ion exchanges with a 1 mol L^{-1} NaCl solution, and the liquid–solid ratio was 50.

3. Results and discussion

3.1. Physical properties of as-synthesized and modified SAPO-17 molecular sieve

As shown in Fig. 1*a*, the XRD pattern of as-synthesized SAPO-17 showed strong diffraction peaks in good agreement with the simulated pattern of the ERI zeolite derived from the single-crystal structural data, indicating that SAPO-17 was prepared with high crystallinity and purity. The XRD patterns of H-SAPO-17 and Na-SAPO-17 showed that calcination and ion exchange did not change the structure of the molecular sieve material, revealing the good thermal and hydrothermal stability of SAPO-17 molecular sieve.

Fig. 2. (*a*) Pure component adsorption isotherms of H-SAPO-17 at 298 K and DSL-F model fitting results; (*b*) pure component adsorption isotherms of Na-SAPO-17 at 298 K and DSL-F model fitting results; (*c*) adsorption amount of propylene on H-SAPO-17 and Na-SAPO-17 regenerated at 298 K in vacuum; (*d*) ^{1}H NMR spectra of H-SAPO-17 and Na-SAPO-17. [Colour online.]

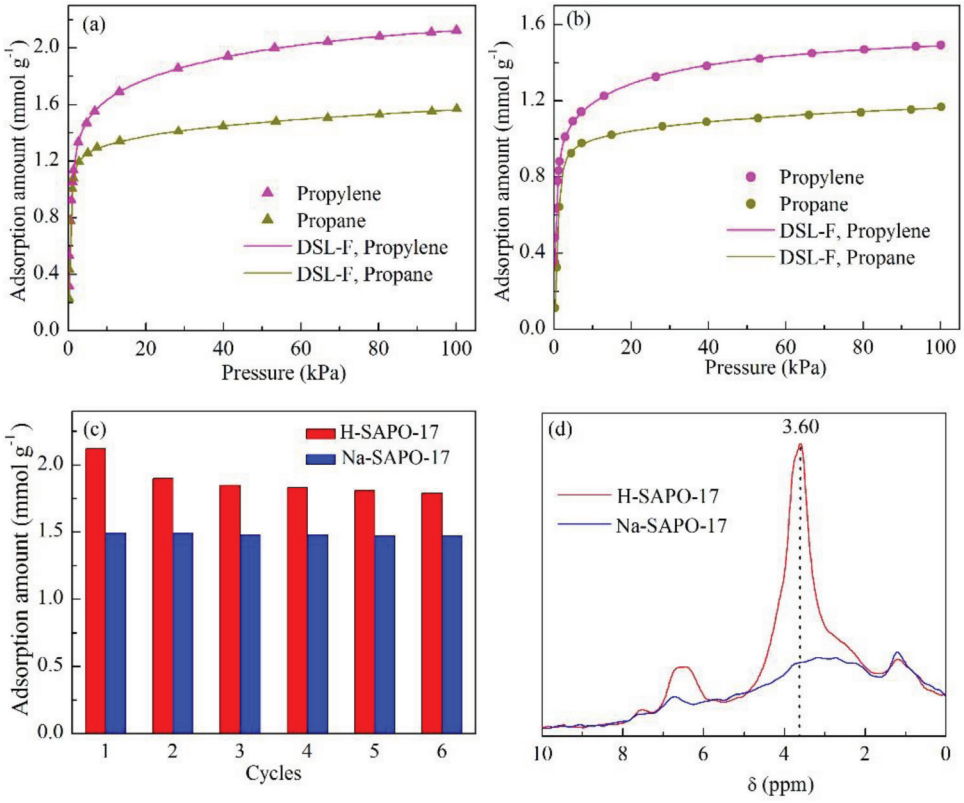

Compared with the XRD pattern of as-synthesized SAPO-17 molecular sieve, the diffraction peaks of H-SAPO-17 moved to a higher field in the range of 0.25 degree, which indicated that after the removal of organic templates, the cell shrank slightly. The diffraction peak positions of Na-SAPO-17 coincided with those of H-SAPO-17, meaning that ion exchange treatment did not make big difference in the cell parameters of SAPO-17 molecular sieve.

As shown in Fig. 1*b*, the isothermal curves of H-SAPO-17 and Na-SAPO-17 were both type I for microporous materials. Both H-SAPO-17 and Na-SAPO-17 had large micropore areas and volumes, as shown in Table 1. Compared with H-SAPO-17, the micropore area and volume of Na-SAPO-17 were relatively small, indicating that sodium ions occupied more microporous space than protons. The chemical compositions of the H-SAPO-17 and Na-SAPO-17 were given in Supplementary Table S4.

3.2. Static adsorption and regeneration behavior

As shown in Fig. 2*a*, the adsorption capacities of propylene and propane on H-SAPO-17 molecular sieve were 2.12 and 1.57 mmol g^{-1}, respectively, at 100 kPa and 298 K. At a low pressure region (<2 kPa), the adsorption amounts of propylene or propane increased rapidly. As the pressure grew in the high pressure region, the adsorption amounts increased slowly and approached the adsorption capacities. After the ion exchange treatment, as shown in Fig. 2*b*, the adsorption capacities of propylene and propane on Na-SAPO-17 reduced to 1.49 and 1.17 mmol g^{-1}, which could be attributed to the reduction of micropore volume, as shown in Table 1. The adsorption isotherm data of propylene and propane were fitted using the dual-site Langmuir–Freundlich (DSL-F) model[25] with correlation coefficient (R^2) > 0.999, as shown in Supplementary Table S1.

To evaluate the regeneration performance of H-SAPO-17 and Na-SAPO-17 in propylene/propane separation, the regeneration and adsorption of propylene was repeated five times (Fig. 2*c*). The propylene adsorption capacity of H-SAPO-17 decreased obviously (1.90 mmol g^{-1}) after the first regeneration and kept decreasing in the following regeneration cycles, indicating that a certain amount of propylene was strongly adsorbed on H-SAPO-17 and could not release after vacuum treatment. However, the initial propylene adsorption capacity of Na-SAPO-17 could be completely restored in each cycle, which indicated that there is no strong interaction between propylene and Na-SAPO-17, and the propylene molecule could thoroughly desorb from adsorbent in vacuum at room temperature.

It was reported that propylene would strongly adsorb on bridging acid hydroxyl groups of Brönsted acids by forming π-complexes with a strong hydrogen bond.[26,27] As a result, Brönsted acids catalyzed the oligomerization of propylene even at room temperature, and the products would be converted to carbonaceous compounds during the regeneration process, which would block the access of adsorbates to the molecular sieve pores.[28] As shown in Fig. 2*d*, the ^{1}H NMR spectra of H-SAPO-17 showed a strong peak at 3.60 ppm, which was attributed to the protons in bridging hydroxyl groups as Brönsted acid sites. The calculated concentration of Brönsted acid sites in H-SAPO-17 was 0.101 mmol g^{-1}. After ion exchange, the intensity of the peak at 3.60 ppm decreased substantially, indicating that the protons in the bridging hydroxyl groups were almost completely replaced by sodium ions; thus, Brönsted acid sites in the SAPO-17 molecular sieve were almost eliminated.

The IR characterization results (Supplementary Fig. S2) showed that the propylene molecule strongly adsorbed on the H-SAPO-17, changing the concentration of Brönsted acid sites of the adsorbent obviously, and a certain amount of propylene could not desorb

Fig. 3. Kinetic adsorption curves of propylene and propane on Na-SAPO-17 at 298 K and 2 mbar. [Colour online.]

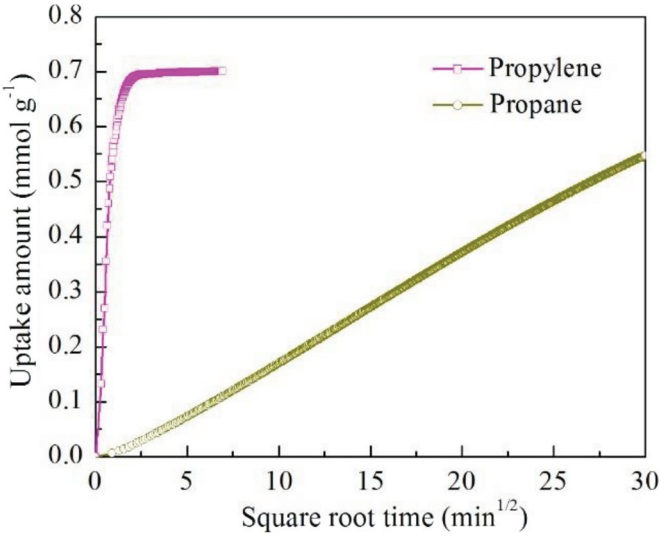

after vacuum treatment. Although Supplementary Fig. S3 showed that the concentration of Brönsted acid sites of Na-SAPO-17 was very low, the propylene desorbed from Na-SAPO-17 almost completely after vacuum treatment. The detailed discussion was shown in Supplementary Fig. S3. Therefore, the decrease of adsorption amount of propylene on H-SAPO-17 in Fig. 2*c* was mainly due to the strong interaction between propylene molecule and the Brönsted acid sites in the H-SAPO-17 framework.

3.3. Dynamic adsorption

The static adsorption results showed that SAPO-17 has low equilibrium selectivity for propylene and propane separation. However, it was observed that the adsorption equilibrium time of propylene was much shorter than that of propane in the statistic adsorption experiment, so it was reasonable to speculate that the sample might have high kinetic selectivity in propylene/propane separation. The adsorption rates of propane and propylene on Na-SAPO-17 material were measured by the dynamic gravimetric method, and the results were shown in Fig. 3. The adsorption amount of propylene increased rapidly at the initial contact with the adsorbent Na-SAPO-17 and reached equilibrium in 10 min, which indicated that restriction of propylene diffusing through the channels of molecular sieve was weak. However, the adsorption amount of propane increased slowly, and adsorption equilibrium took more than 7000 min. At 5 min, the propylene adsorption amount was 0.69 mmol g^{-1} (98.8% of the equilibrium adsorption capacity), whereas the propane amount was only 2.6% of the saturated adsorption capacity at the same time. SAPO-17 has elliptical channels with a size of 3.6 Å × 5.1 Å, which is close to the kinetic diameters of propylene and propane.[2] The cross-section of propylene is slightly smaller than propane,[29] so it is easier for propylene to diffuse through the elliptical channel, which is the direct reason for the dynamic experimental phenomena.

The diffusion time constants (D/r^2) were calculated by short-time solution of the diffusion equation[30] based on following assumptions: (*i*) the diffusion was controlled by micropores, (*ii*) the adsorption bed was clean, and (*iii*) there was a step change in the concentration of gas phase.

$$(1) \qquad \frac{q_t}{q_\infty} = \frac{6}{\sqrt{\pi}}\sqrt{\frac{D}{r^2}t}$$

Table 2. Diffusion time constants for propylene and propane and kinetic selectivity on adsorbents.

Material	Temperature (K)	D/r^2 (s^{-1}) Propylene	Propane	Kinetic selectivity
ITQ-3[17]	303	1.5×10^{-3}	2.2×10^{-6}	690
ITQ-32[19]	298	3.86×10^{-5}	2.7×10^{-8}	1 430
ZSM-58[17]	303	1.2×10^{-4}	9.6×10^{-9}	12 400
Si-CHA[17]	303	4.6×10^{-4}	1.0×10^{-8}	46 000
ITQ-12[18]	353	5.6×10^{-2}	2.0×10^{-8}	2 800 000
SAPO-17	298	1.08×10^{-3}	5.45×10^{-7}	1 980

Table 3. Calculated van der Waals energy, valence bond energy, and potential energy in the cage and in the ring for propane and propylene.

Position	E_{vdW} (kJ mol^{-1})	E_v (kJ mol^{-1})	E_p (kJ mol^{-1})
Propane			
Cage	−31.5	0	−31.5
Ring	26.3	9.6	35.9
Propylene			
Cage	−28.1	0	−28.1
Ring	14.2	0.1	14.2

Note: The energy barriers (E_b, kJ mol^{-1}) for propane and propylene were 67.4 and 42.3, respectively.

where q_t (mmol g^{-1}) is the adsorption amount at time t (s), q_∞ (mmol g^{-1}) is the equilibrium adsorption amount, D (m^2 s^{-1}) is the diffusivity, and r (m) is the radius of the equivalent spherical particle.

The kinetic selectivity of propylene and propane was defined as the ratio of their diffusion time constants, as given in Table 2. The adsorbent Na-SAPO-17 had acceptable kinetic selectivity (1980) for separation of propylene/propane mixtures. More importantly, the adsorbent had a fast kinetic of propylene adsorption, i.e., propylene could diffuse into the pores fast; thus, the separation process on Na-SAPO-17 was practical from an industrial standpoint.[29]

3.4. Molecular simulation

To get further insight into the diffusion of propylene and propane into the SAPO-17 adsorbent, this process was studied through molecular simulation based on Monte Carlo method. As described by Horst,[31] the diffusion coefficient of adsorbate was determining by energy barrier (E_b) when it diffused through the eight-membered ring, which was the potential energy difference when adsorbate in the minimum energy and maximum energy positions, namely in the cage ($E_{p,cage}$) and in the ring ($E_{p,ring}$).

$$(2) \qquad E_b = E_{p,ring} - E_{p,cage}$$

The total potential energy consisted of van der Waals energy (E_{vdW}) and valence bond energy (E_v). The theoretical calculation details were shown in Supplementary Fig. S5, and results were given in Table 3. The van der Waals energy of propane was similar to propylene when they were in the cage, but it was higher than the latter in the ring. To pass through the eight-membered ring, propane would adjust its bond angle from 113° to 123°, leading to a rise in valence bond energy. Propylene's bond angle (120°) did not change significantly, so its valence bond energy remained almost unchanged. As a result, the energy barrier of propane (67.4 kJ mol^{-1}) to diffuse through the eight-membered ring was much higher than that of propylene (42.3 kJ mol^{-1}). The diffusion coefficient of propane was much smaller than propylene, which was in good agreement with the dynamic adsorption results.

Fig. 4. (*a*) Breakthrough curves of fresh Na-SAPO-17 and Na-SAPO-17 regenerated for different amounts of time. (*b*) Breakthrough curves of Na-SAPO-17 regenerated for 24 h repeatedly. Closed symbols, propylene; open symbols, propane. [Colour online.]

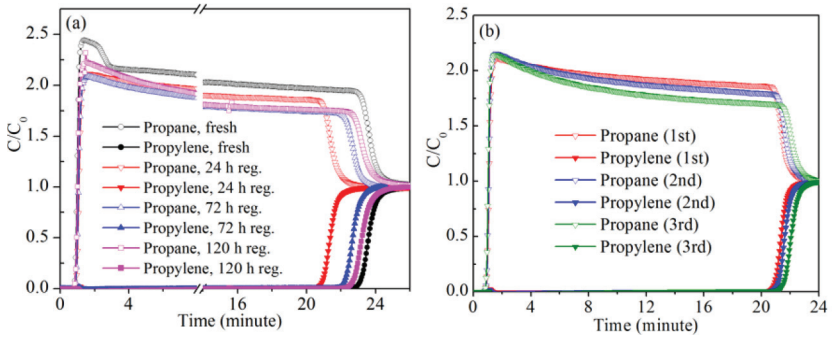

3.5. Breakthrough experiments

The kinetic separation performance of propylene and propane was verified by breakthrough experiments. As shown in Fig. 4*a*, propane started penetrating the adsorbent bed at 50 s, and the concentration reached the maximum immediately; the adsorption amount was equivalent to 0.95 mL g^{-1}. Controlled by kinetic diffusion, the inner surface and pore of the molecular sieve adsorbent was inaccessible to propane, and adsorption occurred only on the outer surface of the adsorbent, so only a small amount of propane molecules were adsorbed after short-term contact. However, the penetration time of propylene was up to 22.7 min, and the adsorption amount was equivalent to 25.9 mL g^{-1}. Because the restriction of propylene diffusing through the channels of molecular sieve was weak, propylene could diffuse through the microchannels easily. Therefore, although the equilibrium adsorption capacities of propylene and propane were close, due to the kinetic factor, the adsorption capacity of propylene was much higher than that of propane in the dynamic breakthrough experiment, showing excellent separation performance. The binary uptake ratio α(propylene/propane) was as high as 27.

After regeneration for 24 h by helium purging at room temperature, the penetration time of propylene was 20.6 min, and 91% of the adsorption capacity was restored. On the other hand, the penetration time of propane on regenerated Na-SAPO-17 was exactly same as that on fresh sample, confirming that propane was mainly adsorbed on the outer surface. As shown in Fig. 4*b*, the regeneration and adsorption experiments were repeated for two additional cycles, and the results were consistent with the first experiment within the range of experimental errors, indicating that the adsorption and desorption processes did not generate any carbonaceous compounds, which would block the access of propylene to the molecular sieve pores. As the regeneration time increased to 72 and 120 h, the propylene's penetration time recovered to 21.9 and 22.5 min, respectively. As the regeneration time increased, the kinetic separation performance was restored almost completely, and 99% of the adsorption capacity was restored after 120 h helium purging. Combined the results of the pure component equilibrium adsorption and breakthrough experiments, it could be seen that the ion-exchange SAPO-17 molecular sieve exhibited excellent kinetic separation performance for propylene and propane, as well as good regeneration behavior at room temperature.

4. Conclusion

In conclusion, SAPO-17 molecular sieve exhibited good performance for propylene/propane separation. The kinetic selectivity of the Na-SAPO-17 molecular sieve for propylene and propane was as high as 1980, the binary breakthrough adsorption amount ratio was 27. The energy barrier of adsorbate molecule diffusing through the eight-membered ring was the main reason for the high kinetic selectivity of propylene and propane. Ion exchange treatment could efficiently eliminate Brönsted acid sites of H-SAPO-17 and weaken the strong interaction between adsorbents and propylene molecular, so the adsorption of propylene on the Na-SAPO-17 molecular sieve became reversible. The study suggested that SAPO-17 has considerable application potential in the separation of propylene and propane.

Supplementary data

Supplementary data are available with the article at https://doi.org/10.1139/cjc-2020-0489.

References

(1) Faiz, R.; Li, K. *Chem. Eng. Sci.* **2012**, 73, 261. doi:10.1016/j.ces.2012.01.037.
(2) Wang, Y.-X.; Peh, S. B.; Zhao, D. *Small.* **2019**, 15, 1900058. doi:10.1002/smll.201900058.
(3) Sholl, D. S.; Lively, R. P. *Nature.* **2016**, 532, 435. doi:10.1038/532435a.
(4) Yu, B.-Y.; Chien, I. L. *Chem. Eng. Technol.* **2016**, 39, 2304. doi:10.1002/ceat.201600168.
(5) Cadiau, A.; Adil, K.; Bhatt, P. M.; Belmabkhout, Y.; Eddaoudi, M. *Science.* **2016**, 353, 137. doi:10.1126/science.aaf6323.
(6) Peng, J.; Wang, H.; Olson, D. H.; Li, Z.; Li, J. *Chem. Commun.* **2017**, 53, 9332. doi:10.1039/C7CC03529B.
(7) Ruthven, D. M. *Chem. Eng. Prog.* **1988**, 84, 42.
(8) Wang, Y.; Zhao, D. *Growth Des.* **2017**, 17, 2291. doi:10.1021/acs.cgd.7b00287.
(9) Yang, R. T. 2003, Adsorbents: Fundamentals and Applications; *Edited by* John Wiley & Sons: Hoboken. pp. 131–156.
(10) Silva, F. A. D.; Rodrigues, A. E. *Ind. Eng. Chem. Res.* **1999**, 38, 2051. doi:10.1021/ie980640z.
(11) Lamia, N.; Wolff, L.; Leflaive, P.; Leinekugel-Le-Cocq, D.; Gomes, P.S.; Grande, C. A.; Rodrigues, A. E. *Sep. Sci. Technol.* **2008**, 43, 1124. doi:10.1080/01496390801888136.
(12) Silva, F. A. D.; Rodrigues, A. E. *AIChE J.* **2001**, 47, 341. doi:10.1002/aic.690470212.
(13) Gomes, P. S.; Lamia, N.; Rodrigues, A. E. *Chem. Eng. Sci.* **2009**, 64, 1336. doi:10.1016/j.ces.2008.11.022.
(14) Grande, C. A.; Gigola, C.; Rodrigues, A. E. *J. Int. Adsorpt. Soc.* **2003**, 9, 321. doi:10.1023/A:1026223914143.
(15) Zhu, W.; Kapteijn, F.; Moulijn, J. A.; Den Exter, M. C.; Jansen, J. C. *Langmuir.* **2000**, 16, 3322. doi:10.1021/la9914007.
(16) Gascon, J.; Blom, W.; Miltenburg, A. V.; Ferreira, A.; Berger, R.; Kapteijn, F. *Microporous Mesoporous Mater.* **2008**, 115, 585. doi:10.1016/j.micromeso.2008.02.038.
(17) Olson, D. H.; Camblor, M. A.; Villaescusa, L. A.; Kuehl, G. H. *Microporous Mesoporous Mater.* **2004**, 67, 27. doi:10.1016/j.micromeso.2003.09.025.
(18) Barrett, P. A.; Boix, T.; Puche, M.; Olson, D. H.; Jordan, E.; Koller, H.; Camblor, M. A. *Chem. Commun.* **2003**, 17, 2114.
(19) Palomino, M.; Cantin, A.; Corma, A.; Leiva, S.; Rey, F.; Valencia, S. *Chem. Commun.* **2007**, 12, 1233.
(20) Padin, J.; Rege, S. U.; Yang, R. T.; Cheng, S. *Chem. Eng. Sci.* **2000**, 55, 4525. doi:10.1016/S0009-2509(00)00099-3.
(21) Hong, M.; Li, S.; Funke, H. F.; Falconer, J. L.; Noble, R. D. *Microporous Mesoporous Mater.* **2007**, 106, 140. doi:10.1016/j.micromeso.2007.02.037.
(22) Grande, C. A.; Gascon, J.; Kapteijn, F.; Rodrigues, A. E. *Chem. Eng. J.* **2010**, 160, 207. doi:10.1016/j.cej.2010.03.044.
(23) Database of Zeolite Structures, The International Zeolite Association. (http://www.iza-structure.org/databases) (Accessed 1 December 2020).
(24) Lok B. M. U.S. Patent 4440871, Apr 3. 1984.

(25) Sips, R; J. *Chem. Phys.* **1948**, 16, 490J.
(26) Subbotina, I. R.; Kazanskii, V. B. *Kinet. Catal.* **2002**, 43, 115. doi:10.1023/A:1014265500045.
(27) Ghosh, A. K.; Kydd, R. A. *J. Catal.* **1986**, 100, 185. doi:10.1016/0021-9517(86)90084-9.
(28) Boucheffa, Y.; Thomazeau, C.; Cartraud, P.; Magnoux, P.; Guisnet, M.; Jullian, S. *Ind. Eng. Chem. Res.* **1997**, 36, 3198. doi:10.1021/ie960646t.
(29) Bryan, P. F. *Purif. Rev.* **2004**, 33, 157. doi:10.1081/SPM-200042095.
(30) Lee, C. Y.; Bae, Y. S.; Jeong, N. C.; Farha, O. K.; Sarjeant, A. A.; Stern, C. L.; Nickias, P.; Snurr, R.Q.; Hupp, J.T.; Nguyen, S.T. *J. Am. Chem. Soc.* **2011**, 133, 5228. doi:10.1021/ja200553m.
(31) ter Horst, J. H.; Bromley, S. T.; van Rosmalen, G. M.; Jansen, J. C. *Microporous Mesoporous Mater.* **2002**, 53, 45. doi:10.1016/S1387-1811(02)00323-2.